Two hydrates of 2,6-bis(1*H*-benzimidazol-2-yl)pyridine

Eleonora Freire,[a] Sergio Baggio,[a] Juan Carlos Muñoz[b] and Ricardo Baggio[c]*

[a]Universidad Nacional de la Patagonia, Sede Puerto Madryn, and CenPat, CONICET, 9120 Puerto Madryn, Chubut, Argentina, [b]Departamento de Física, Facultad de Ciencias Físicas y Matemáticas, Universidad de Chile, Casilla 487-3, Santiago de Chile, Chile, and [c]Departamento de Física, Comisión Nacional de Energía Atómica, Buenos Aires, Argentina
Correspondence e-mail: baggio@cnea.gov.ar

The structures of the mono- and sesquihydrates of 2,6-bis(1*H*-benzimidazol-2-yl)pyridine (bbip) are reported. Phase (I), $C_{19}H_{13}N_5 \cdot H_2O$, has one water and one bbip molecule in the asymmetric unit, while phase (II), $C_{19}H_{13}N_5 \cdot 1.5H_2O$, has three water molecules and two bbip molecules in the asymmetric unit. The compounds exhibit very similar molecular geometries but different packing organizations, which result from intricate hydrogen-bonding schemes.

Comment

During the past decade we have been carrying out a systematic study of the crystal structures of metal–thiosulfate compounds. By changing the size and/or the coordination sites of some accompanying *N*-polydentate organic ligands, we expected that useful information about their influence on the binding of the anion to the metal would be revealed. Through this strategy, we have been able to investigate a large number of thiosulfate complexes based on the most common *N*,*N'*-bidentate ligands, including 2,2'-bipyridine (Freire *et al.*, 1999; Baggio *et al.*, 1997*b*,*c*; Freire, Baggio, Baggio & Mariezcurrena, 2000), 1,10-phenanthroline (Freire *et al.*, 1999, 2001; Baggio *et al.*, 1996*a*, 1998; Freire, Baggio, Baggio & Mariezcurrena, 2000) and 2,9(or 4,7)-dimethyl-1,10-phenanthroline (Baggio *et al.*, 1996*b*, 1997*a*; Freire, Baggio, Suescun & Baggio, 2000).

As a natural extension of this project, we decided to include *N*,*N'*,*N''*-tridentate ligands in the compounds under study. Among molecules deemed potentially suitable for our purposes, we focused our attention and efforts on 2,6-bis-(benzimidazol-2-yl)pyridine (hereafter bbip), which has been studied less than other common *N*,*N'*,*N''*-tridentate species (*e.g.* terpyridine *etc.*). A search of the November 2002 release of the Cambridge Structural Database (CSD; Allen, 2002)

showed 12 entries in which the molecule acts as a tridentate ligand and complexes with different metals, and another two in which the molecule does not coordinate, *viz.* hydroxy-triphenyltin 2,6-bis(1*H*-benzimidazol-2-yl)pyridine monohydrate (Lo *et al.*, 1999), in which bbip acts as a neutral moiety, and 2-[6-(1*H*-benzimidazol-2-yl)-2-pyridyl]-1*H*-benzimidazol-3-ium perchlorate monohydrate (Boča *et al.*, 2000), in which bbip acts as a singly protonated ion.

$\cdot H_2O$, (I)
$\cdot 1.5H_2O$, (II)
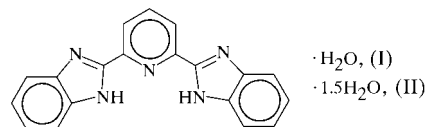
During the synthesis of a variety of bbip–thiosulfate complexes, we obtained, as unexpected by-products, well shaped crystals that were suspected to be two different hydrated phases of free bbip. The lack of pure bbip hydrates in the CSD, as well as our interest in the free molecules for comparison with those in our synthesized complexes (to be reported elsewhere), prompted us to undertake structural studies of these crystals, which are reported here.

Both forms crystallize in the monoclinic space group $P2_1/c$, but while monohydrate phase (I) contains one bbip and one water molecule in each asymmetric unit (Fig. 1), sesquihydrate phase (II) contains three water and two independent bbip molecules (Fig. 2). The molecular structures do not depart from the expected structures, and they exhibit quite similar bond distances and angles (Tables 1 and 3); with very few exceptions, corresponding parameters in the two structures fall within one standard deviation of one another. The main differences in the molecular geometries arise from the slight rotation of the lateral wings around the C7—C8 and C12—C13 single bonds, under the strains imposed by extensive hydrogen-bonding interactions. In both structures, all the H atoms amenable to hydrogen bonding are involved in these kinds of interactions, leading, in both cases, to tightly woven networks.
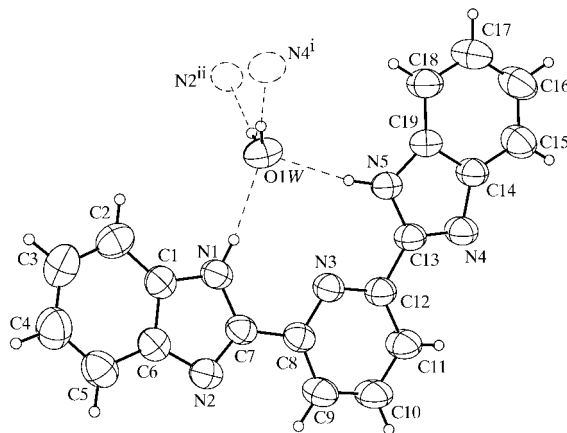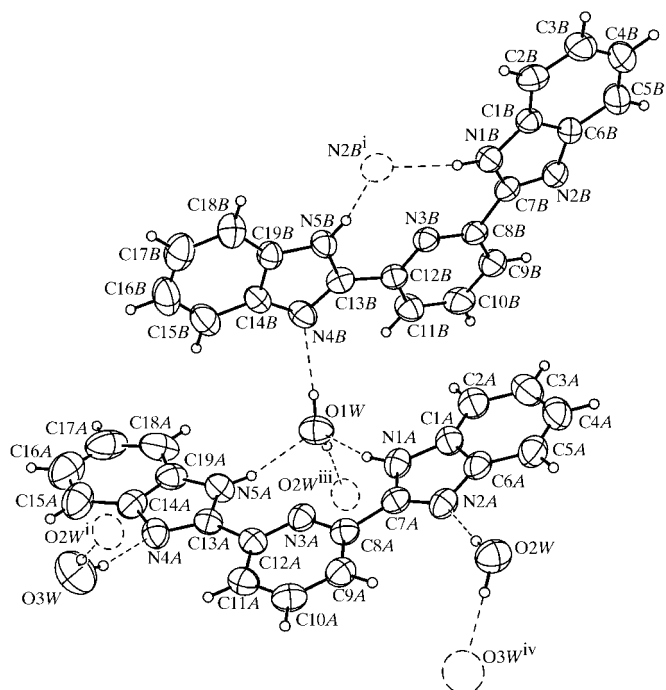

Figure 1
An *XP* (Sheldrick, 1994) view of (I), showing the atom-numbering scheme and hydrogen-bonding interactions. Displacement ellipsoids are shown at the 50% probability level. [Symmetry codes: (i) $x, \frac{3}{2} - y, \frac{1}{2} + z$; (ii) $x - 1, y, z$.]
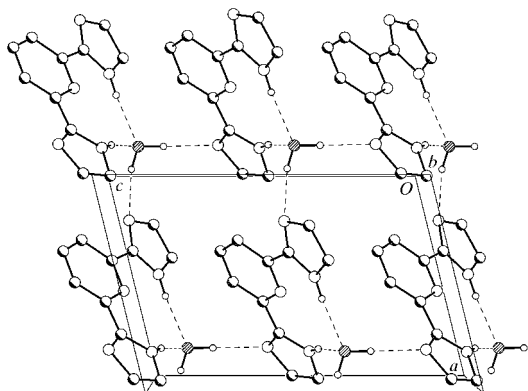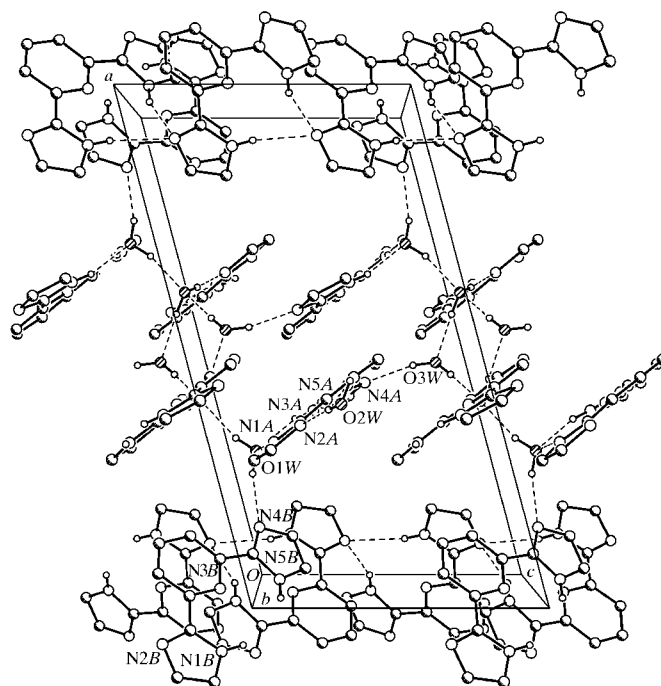
Figure 2
An *XP* (Sheldrick, 1994) view of (II), showing the atom-numbering scheme and hydrogen-bonding interactions. Displacement ellipsoids are shown at the 50% probability level. [Symmetry codes: (i) x, $\frac{3}{2} - y$, $\frac{1}{2} + z$; (iii) x, $\frac{3}{2} - y$, $z - \frac{1}{2}$; (iv) $1 - x$, $\frac{1}{2} + y$, $\frac{3}{2} - z$.]

In (I), the only water molecule present in the structure acts as a donor of its two H atoms (accepted by the unprotonated N atoms of two different bbip molecules) and as an acceptor of the H atom of the protonated amine N atom of a third bbip unit. The water molecule thus acts as a central link for the packing interactions, which build broad two-dimensional structures parallel to the (010) plane (Table 2, and Figs. 1 and 3) at $y \simeq \frac{1}{4}$ and $\frac{3}{4}$. There is, in addition, a π-stacking interaction, which provides a link between layers and which connects the benzimidazolyl group (N1/N2/C1–C7) with its $(1 - x, 1 - y, 1 - z)$ centrosymmetric image. The two parallel groups are separated by ~3.4 Å, with an estimated overlap of 30% of their areas.

Figure 3
A view of the packing of (I). For clarity, neither the lateral wings of the bbip molecule nor H atoms attached to C atoms are shown.

Figure 4
A view of the packing of (II). For clarity, neither the lateral wings of the bbip molecule nor H atoms attached to C atoms are shown.

The packing of (II) is more complicated. There are two different types of hydrogen-bonded aggregate, each involving only one of the two independent bbip molecules present (Table 4, and Figs. 2 and 4). One molecule, bbip(A), interacts with all three water molecules to form a two-dimensional network parallel to the (100) plane at $x \simeq \frac{1}{2}$. The central knot is a closed loop, built around a center of inversion, which involves the O2W and O3W water molecules and to which molecule bbip(A) bonds through the acceptance of one H atom from each of the O2W and O3W water molecules. Molecule bbip(A) also chelates, with hydrogen bonds, the remaining water molecule, O1W, which in turn donates one hydrogen bond to the central knot. On the other hand, molecule bbip(B) is involved in a chain structure, which evolves parallel to the [001] direction and is the result of a pure bbip···bbip interaction that is not mediated by water. Finally, the compact two-dimensional structure formed by the bbip(A) molecules and the set of parallel chains containing the bbip(B) molecules link together through water molecule O1W, which is already involved in the two-dimensional bbip(A) network and which donates its remaining hydrogen bond to the basic N4B atom. No stacking interactions were found for the bbip(B) aggregate. In the bbip(A) aggregate, the N3A/C8A–C12A pyridyl ring exhibits a parallel overlap of ~90% of its total area with the N1A/N2A/C1A–C7A benzimidazolyl group, these groups being related by $(x, \frac{3}{2} - y, -\frac{1}{2} + z)$, with a mean distance of ~3.30 Å between their planes. In addition, the operation $(1 - x, 1 - y, 1 - z)$ generates two parallel images of the N3A/N4A/N5A/C8A–C19A pyridylbenzimidazolyl group, which are separated by ~3.45 Å and exhibit a small overlap (~15%).

Comparison of (I) and (II) with other compounds containing bbip shows that the most significant differences occur in the torsion angles around the C—C single bonds, all other parameters being almost the same. The structures presented here share with the only free neutral bbip example (Lo *et al.*, 1999) a *trans–trans* disposition of atoms N2 and N4 with respect to atom N3 (N2—C7—C8—N3 and N3—12—C13—N4 $\simeq$ 180°). When chelating to a metal, the ligand reverses the orientation of the benzimidazolyl wings and the relative disposition becomes *cis–cis*, with the corresponding torsion angles being almost zero. However, when considering the relative deviations from 0 or 180°, those in the present structures appear among the largest [8.8 (3)° for (I) and 9.4 (3)° for (IIA)]. These departures from planarity (probably due to hydrogen-bonding strain, as already discussed) are comparable to those in strained bbip moieties coordinated to large cations, for example, bis[2,6-bis(benzimidazol-2-yl)-pyridine-N,N',N'']dinitratocerium(III) (Wang *et al.*, 1994), where bbip exhibits a maximum torsion angle of 8.3 (2)°.

Experimental

Crystals of bbip appeared as a by-product of the synthesis of different metallic bbip–thiosulfate complexes. In these attempted syntheses, the bbip ligand was dissolved in dimethylformamide, while the thiosulfate and metal salts were incorporated as aqueous solutions. On standing, small but well shaped crystals of two differently hydrated species appeared, accompanying the main crop of crystals of the corresponding metal bbip–thiosulfate complex.

Compound (I)

Crystal data

$C_{19}H_{13}N_5 \cdot H_2O$	Mo $K\alpha$ radiation
$M_r = 329.36$	Cell parameters from 102
Monoclinic, $P2_1/c$	reflections
$a = 7.522$ (2) Å	$\theta = 2.1–23.7°$
$b = 20.367$ (3) Å	$\mu = 0.09$ mm^{-1}
$c = 11.264$ (2) Å	$T = 293$ (2) K
$\beta = 103.76$ (2)°	Prism, colorless
$V = 1676.2$ (6) Å^3	$0.18 \times 0.12 \times 0.10$ mm
$Z = 4$	
$D_x = 1.305$ Mg m^{-3}	

Data collection

Bruker SMART CCD area-detector diffractometer	$R_{int} = 0.045$
φ and ω scans	$\theta_{max} = 25.0°$
8338 measured reflections	$h = -8 \rightarrow 8$
2924 independent reflections	$k = -24 \rightarrow 21$
1660 reflections with $I > 2\sigma(I)$	$l = -13 \rightarrow 13$

Table 1
Selected geometric parameters (Å, °) for (I).

N1—C7	1.364 (3)	N4—C13	1.325 (3)
N1—C1	1.374 (3)	N4—C14	1.391 (3)
N2—C7	1.325 (3)	N5—C13	1.361 (3)
N2—C6	1.390 (3)	N5—C19	1.378 (3)
N3—C8	1.333 (2)	C1—C6	1.390 (3)
N3—C12	1.340 (3)		
N2—C7—C8—N3	−171.2 (2)	N3—C12—C13—N4	177.1 (2)

Table 2
Hydrogen-bonding geometry (Å, °) for (I).

D—H$\cdots A$	D—H	H$\cdots A$	$D\cdots A$	D—H$\cdots A$
N1—H1N$\cdots$O1W	0.90 (2)	2.13 (2)	3.019 (3)	172 (2)
N5—H5N$\cdots$O1W	0.91 (2)	2.10 (2)	3.006 (3)	170 (2)
O1W—H1$WB\cdots$N4^i	0.92 (2)	2.01 (2)	2.922 (3)	173 (2)
O1W—H1$WA\cdots$N2^{ii}	0.93 (2)	2.01 (2)	2.926 (3)	167 (2)

Symmetry codes: (i) $x, \frac{3}{2} - y, \frac{1}{2} + z$; (ii) $x - 1, y, z$.

Refinement

Refinement on F^2	$w = 1/[\sigma^2(F_o^2) + (0.0454P)^2]$
$R[F^2 > 2\sigma(F^2)] = 0.048$	where $P = (F_o^2 + 2F_c^2)/3$
$wR(F^2) = 0.119$	$(\Delta/\sigma)_{max} = 0.007$
$S = 0.91$	$\Delta\rho_{max} = 0.16$ e Å^{-3}
2924 reflections	$\Delta\rho_{min} = -0.15$ e Å^{-3}
243 parameters	
H atoms treated by a mixture of independent and constrained refinement	

Compound (II)

Crystal data

$C_{19}H_{13}N_5 \cdot 1.5H_2O$	$D_x = 1.300$ Mg m^{-3}
$M_r = 338.37$	Mo $K\alpha$ radiation
Monoclinic, $P2_1/c$	Cell parameters from 154
$a = 18.813$ (2) Å	reflections
$b = 18.417$ (2) Å	$\theta = 3.1–24.5°$
$c = 10.322$ (2) Å	$\mu = 0.09$ mm^{-1}
$\beta = 104.81$ (2)°	$T = 293$ (2) K
$V = 3457.5$ (8) Å^3	Prism, colorless
$Z = 8$	$0.16 \times 0.10 \times 0.08$ mm

Data collection

Bruker SMART CCD area-detector diffractometer	$R_{int} = 0.064$
φ and ω scans	$\theta_{max} = 25.0°$
17 546 measured reflections	$h = -21 \rightarrow 22$
6086 independent reflections	$k = -21 \rightarrow 18$
2514 reflections with $I > 2\sigma(I)$	$l = -12 \rightarrow 12$

Refinement

Refinement on F^2	$w = 1/[\sigma^2(F_o^2) + (0.0202P)^2]$
$R[F^2 > 2\sigma(F^2)] = 0.046$	where $P = (F_o^2 + 2F_c^2)/3$
$wR(F^2) = 0.087$	$(\Delta/\sigma)_{max} = 0.010$
$S = 0.88$	$\Delta\rho_{max} = 0.16$ e Å^{-3}
6086 reflections	$\Delta\rho_{min} = -0.16$ e Å^{-3}
501 parameters	
H atoms treated by a mixture of independent and constrained refinement	

Table 3
Selected bond lengths (Å) for (II).

N1A—C7A	1.363 (3)	N1B—C7B	1.357 (3)
N1A—C1A	1.372 (4)	N1B—C1B	1.372 (3)
N2A—C7A	1.325 (3)	N2B—C7B	1.316 (3)
N2A—C6A	1.392 (4)	N2B—C6B	1.403 (3)
N3A—C12A	1.331 (3)	N3B—C8B	1.332 (3)
N3A—C8A	1.344 (3)	N3B—C12B	1.339 (3)
N4A—C13A	1.317 (3)	N4B—C13B	1.312 (3)
N4A—C14A	1.395 (3)	N4B—C14B	1.392 (3)
N5A—C13A	1.351 (4)	N5B—C13B	1.361 (3)
N5A—C19A	1.377 (4)	N5B—C19B	1.371 (3)

organic compounds

Table 4
Hydrogen-bonding geometry (Å, °) for (II).

$D—H\cdots A$	$D—H$	$H\cdots A$	$D\cdots A$	$D—H\cdots A$
N1A—H1N$A\cdots$O1W	0.94 (2)	2.03 (2)	2.946 (4)	164 (3)
N5A—H5N$A\cdots$O1W	0.88 (2)	2.05 (2)	2.907 (4)	166 (3)
N1B—H1N$B\cdots$N2B^{i}	0.90 (2)	2.47 (2)	3.353 (4)	167 (2)
N5B—H5N$B\cdots$N2B^{i}	0.89 (2)	2.21 (2)	3.048 (3)	157 (2)
O1W—H1W$A\cdots$O2W^{iii}	0.90 (3)	1.88 (3)	2.758 (4)	164 (3)
O1W—H1W$B\cdots$N4B	0.90 (3)	2.04 (3)	2.914 (4)	163 (3)
O2W—H2W$A\cdots$N2A	0.88 (3)	1.92 (3)	2.800 (4)	175 (3)
O2W—H2W$B\cdots$O3W^{iv}	0.87 (3)	1.91 (3)	2.780 (4)	176 (4)
O3W—H3W$A\cdots$N4A	0.88 (2)	1.93 (2)	2.791 (4)	166 (4)
O3W—H3W$B\cdots$O2W^{i}	0.89 (5)	2.03 (5)	2.905 (4)	171 (4)

Symmetry codes: (i) $x, \frac{3}{2} - y, \frac{1}{2} + z$; (iii) $x, \frac{3}{2} - y, z - \frac{1}{2}$; (iv) $1 - x, \frac{1}{2} + y, \frac{3}{2} - z$.

In spite of their good external appearance, the crystals were of poor diffracting power, as can be assessed by the low $N_{\text{obs}}/N_{\text{uniq}}$ ratio, and hence the data sets were chopped at a 2θ angle of 50°. H atoms attached to C atoms were added at expected positions and treated as riding. H atoms attached to water molecules and to the protonated N atoms in bbip were found in the final difference Fourier map and refined with restrained N—H (0.85 Å), O—H (0.90 Å) and H$\cdots$H (1.66 × O—H) distances.

For both compounds, data collection: *SMART-NT* (Bruker, 2001); cell refinement: *SMART-NT*; data reduction: *SAINT-NT* (Bruker, 2000); program(s) used to solve structure: *SHELXS*97 (Sheldrick, 1997); program(s) used to refine structure: *SHELXL*97 (Sheldrick, 1997); molecular graphics: *XP* in *SHELXTL/PC* (Sheldrick, 1994); software used to prepare material for publication: *SHELXL*97.

Supplementary data for this paper are available from the IUCr electronic archives (Reference: KB1001). Services for accessing these data are described at the back of the journal.

References

Allen, F. H. (2002). *Acta Cryst.* B**58**, 380–388.
Baggio, R., Baggio, S., Pardo, M. I. & Garland, M. T. (1996*a*). *Acta Cryst.* C**52**, 820–823.
Baggio, R., Baggio, S., Pardo, M. I. & Garland, M. T. (1996*b*). *Acta Cryst.* C**52**, 1939–1942.
Baggio, S., Baggio, R. & Garland, M. T. (1998). *Acta Cryst.* C**54**, 1099–1102.
Baggio, S., Pardo, M. I., Baggio, R. & Garland, M. T. (1997*a*). *Acta Cryst.* C**53**, 551–554.
Baggio, S., Pardo, M. I., Baggio, R. & Garland, M. T. (1997*b*). *Acta Cryst.* C**53**, 727–729.
Baggio, S., Pardo, M. I., Baggio, R. & Garland, M. T. (1997*c*). *Acta Cryst.* C**53**, 1570–1572.
Boča, M., Valigura, D., Svoboda, I., Fuess, H. & Linert, W. (2000). *Acta Cryst.* C**56**, 838–839.
Bruker (2000). *SAINT-NT*. Version 6.02a. Bruker AXS Inc., Madison, Wisconsin, USA.
Bruker (2001). *SMART-NT*. Version 5.624. Bruker AXS Inc., Madison, Wisconsin, USA.
Freire, E., Baggio, S., Baggio, R. & Mariezcurrena, R. (2000). *Acta Cryst.* C**56**, 926–929.
Freire, E., Baggio, S., Baggio, R. & Mombru, A. (2001). *Acta Cryst.* C**57**, 14–17.
Freire, E., Baggio, S., Baggio, R. & Suescun, L. (1999). *Acta Cryst.* C**55**, 1780–1784.
Freire, E., Baggio, S., Suescun, L. & Baggio, R. (2000). *Aust. J. Chem.* **53**, 785–790.
Lo, K. M., Kumar Das, V. G. & Ng, S. W. (1999). *Acta Cryst.* C**55**, 1234–1236.
Sheldrick, G. M. (1994). *XP* in *SHELXTL/PC*. Version 4.2. Siemens Analytical X-ray Instruments Inc., Madison, Wisconsin, USA.
Sheldrick, G. M. (1997). *SHELXL*97 and *SHELXS*97. University of Göttingen, Germany.
Wang, S.-X., Zhu, Y., Cui, Y.-X., Wang, L.-F. & Luo, Q.-H. (1994). *J. Chem. Soc. Dalton Trans.* pp. 2523–2530.